

ORIGINAL RESEARCH ARTICLE

Extreme rainfall indices and their consequences on the local farming crop calendar: An agro-climatic zone based study

Enyew Azene Meharie¹, Mintesinot Azene Taye^{1,*}, Adane Tesfaye Lema¹, Melkamu Meseret Alemu²

¹ Institute of Disaster Risk Management and Food Security Studies, Bahir Dar University, Bahir Dar 5501, Ethiopia

² School of Earth Sciences, Bahir Dar University, Bahir Dar 5501, Ethiopia

* Corresponding author: Mintesinot Azene Taye, mintesinotazene@yahoo.com

ABSTRACT

The goal of this study is to investigate the extreme rainfall indices and their consequences on the local farming crop calendar among the agro-climatic zones (ACZs) of the Abiya watershed. Climate Hazards Group Infrared Precipitation (CHIRPS) provided long-term (1981–2019) rainfall data for 50 sample grid points with a spatial resolution of 5×5 km. Different crops are affected differently by the same extreme rainfall event depending on when it occurred and how extreme it was; this means crop calendars for a specific time may be properly governed by extreme climatic conditions. There hasn't been a sufficient published study on extreme rainfall indices and their consequences on crop calendars by considering various ACZ in Ethiopia. The study defined local crop calendar timing and the consequences of the extreme rainfall indices through focus group discussions. INSTAT+ software was applied to calculate eight extreme rainfall indices. The indices were evaluated using Mann-Kendall's (MK) and Sen's slope techniques to identify trends and determine variations in the magnitude, respectively. Increase and decrease indications for various crop calendars were found in each ACZ. Further, going-up signals were seen in the highlands, midlands, and all ACZs for land preparation time (LPT), sowing and management time (SaMT), and harvesting and threshing time (HaTP), respectively. While HaTT was found to be uniform in all ACZs, some of the declining trends in the indices were detected for LPT and SaMT in the cold-highland and highland zones. The perceived trend in indices across the whole ACZ will have direct and unintended consequences for watershed crop production. The findings imply that to reduce the unfavourable consequences of these extreme rainfall occurrences in the agricultural sector, it is necessary to develop suitable crop varieties and drought-tolerant crops, as well as an effective early warning system.

Keywords: agro-climatic zones; climatic hazards; crop calendar; extreme rainfall indices; rain-fed agriculture

1. Introduction

Climate change is causing extreme events all over the world, according to the Intergovernmental Panel on Climate Change's (IPCC) Sixth Assessment Report. Climate extremes are caused by a number of factors, including atmospheric circulation, geography, and human activity^[1]. The frequency and duration of severe events have risen because of climate variability in recent decades, and this trend is expected to continue in the future, leading to extreme ecological reactions^[2,3]. For instance, from 1951 to 2010, there was a significant increase in global rainfall trends (1%–2% per decade)^[4]. The consequences of climate extremes are more severe in unindustrialised countries than in industrialised countries, including Africa^[5].

ARTICLE INFO

Received: 22 September 2023 | Accepted: 7 November 2023 | Available online: 15 November 2023

CITATION

Meharie EA, Taye MA, Lema AT, Alemu MM. Extreme rainfall indices and their consequences on the local farming crop calendar: An agro-climatic zone based study. *Advances in Modern Agriculture* 2023; 4(2): 2312. doi: 10.54517/ama.v4i2.2312

COPYRIGHT

Copyright © 2023 by author(s). *Advances in Modern Agriculture* is published by Asia Pacific Academy of Science Pte. Ltd. This is an Open Access article distributed under the terms of the Creative Commons Attribution License (<https://creativecommons.org/licenses/by/4.0/>), permitting distribution and reproduction in any medium, provided the original work is cited.

Extreme climate events are the leading source of natural catastrophes in East Africa, particularly in Kenya, Ethiopia, and Somalia^[6]. Precipitation predictions indicate an increase across Somalia and a decrease across central and northern Ethiopia^[7]. It is expected that there will be more consecutive dry days and fewer consecutive wet days, respectively^[8]. In recent decades, the extended rains in East Africa have tended to dry out due to natural decadal variability^[9].

The decadal Sea Surface Temperature (SST) variability in the Pacific Ocean can be used to explain regional variations^[10]. The SST variability linked with the El Niño-Southern Oscillation (ENSO) is the most important source of forcing a regular drought in the Horn of Africa^[9]. Within the area, the variations in rainfall amounts are highly related to east-west changes in the zonal Walker circulations that are associated with ENSO^[11]. In comparison, the precipitation rise is due to western Indian Ocean warming^[8].

Ethiopia is one of the states that is affected by climate extremes because of its wide spatial and temporal variation in precipitation and temperature^[12–14]. Changes in the severity of climate extremes have serious consequences for local communities, economies, and the environment^[15,16]. To develop a mitigation and adaptation plan, it is critical to study temporal changes in climate extremes, especially extreme rainfall indices, including their quantity, occurrence, and interval. On the contrary, more days with precipitation and fewer consecutive wet days were detected in different places in Ethiopia^[14,16]. Due to great spatiotemporal variability, there are no stable inclinations in the extreme rainfall indices^[14,16,17].

Facts derived from empirical research^[18] and model studies^[6,19] show that extreme climate phenomena, such as floods and prolonged droughts, have been shifting in terms of frequency, magnitude, timing, and spatial extent. The quantity of wet and dry days, the length of wet and dry times, the amount of rainfall, and the warmest days and nights all change over time^[20,21]. The variation in extreme climate phenomena is different across spatiotemporal scales, and so are the consequences^[22]. In the meantime, the need for information on local-scale climate extreme events has become important in recent times because of the increasing effects of the hazard on agricultural activities. There has been some research on global climate-related extreme occurrences, and their analysis has revealed spatiotemporal variances. Wu et al.^[23] discovered that from 1969–2011, there was an overall drop in the quantity of consecutive dry days and a rise in the annual simple daily intensity index, maximum one-day precipitation, and maximum five-day precipitation.

Former studies^[24–26] conducted a study that focused on an annual scale and revealed the existence of complex trends in extreme rainfalls. This is especially true in mountainous states similar to Ethiopia, where there are notable climatic differences within small horizontal distances, primarily due to complicated topographic places^[27]. Gaining understanding at watershed level has proven difficult because previous climate extreme analyses were primarily conducted at classical (annual, seasonal, and monthly) time scales, which do not align with localised crop calendars for different ACZs. Additionally, the indicated extent of examination would not be proper for creating an adaptation preparation for particular field operations in given ACZs.

In Ethiopia, climatic variables have a greater impact on the timing and distribution of rainfall than the overall amount^[28]. In addition, since the 1970s, risky meteorological conditions have become more prevalent throughout Ethiopia, which has negative consequences for the nation's socio-economic development, its economy governed by agriculture, and the country's main sector, which is heavily reliant on rainfall, both seasonal and annual. The Northwest of Ethiopia is similar in that it experiences unpredictable and erratic rainfall patterns, severe land degradation, extreme poverty, and frequent crop failure^[29]. The Abiya watershed consists of various ACZs and is found in the top part of the Northwest Highlands of Ethiopia. Local farmers faced a variety of issues with their farming operations due to factors related to rainfall variability.

According to Wu et al.^[23], a certain time is ordinarily used to recognise the pattern of a succession of rain drops and their effects, and the choice of time has a significant impact on the results. Furthermore, it has been established that different crops are affected differently by the same extreme rainfall event, depending on when it occurred and how extreme it was^[19]. This means that key field operations or crop calendars for a specific time may be properly governed by extreme climatic conditions. However, there hasn't been a sufficient published study on extreme rainfall indices and their consequences on crop calendars by considering various ACZs in Ethiopia. The Abiya watershed is believed to be a site that can represent the larger context of Northwest Ethiopia and other highlands of the country as well, given its geographic location and composition of ACZs.

Therefore, conducting research at the local level on extreme rainfall indices and how they affect crop calendars at the watershed scale is crucial to giving development agents relevant data on how to implement mitigation and adjustment plans for climate change, improve water resource management, and promote agricultural development. So, analysing extreme rainfall indices and their consequences on the local farming crop calendar in the case of the ACZs of the Abiya Watershed, Northwest Highlands of Ethiopia, is the primary point of the present study.

2. Study area

The investigation is carried out in the Abiya watershed, which is found in northwest Ethiopia within 10°43'0" N to 11°15'0" N latitude and 37°25'0" E to 37°55'0" E longitude, upper Blue Nile basin, Ethiopia (**Figure 1**). The watershed covers an area of 1819 km². Its elevation ranges from 1500 m–4084 m. Following the Ministry of Agriculture^[30], this study adopted the traditional ACZs grouping approach. By using the digital elevation model, the ACZs of the watershed consist of midland, highland, and cold-highland zones. The temperature of the watershed has a mean minimum of 10.7 °C and a mean maximum of 23.7 °C annually. The mean annual rainfall was 1324 mm.

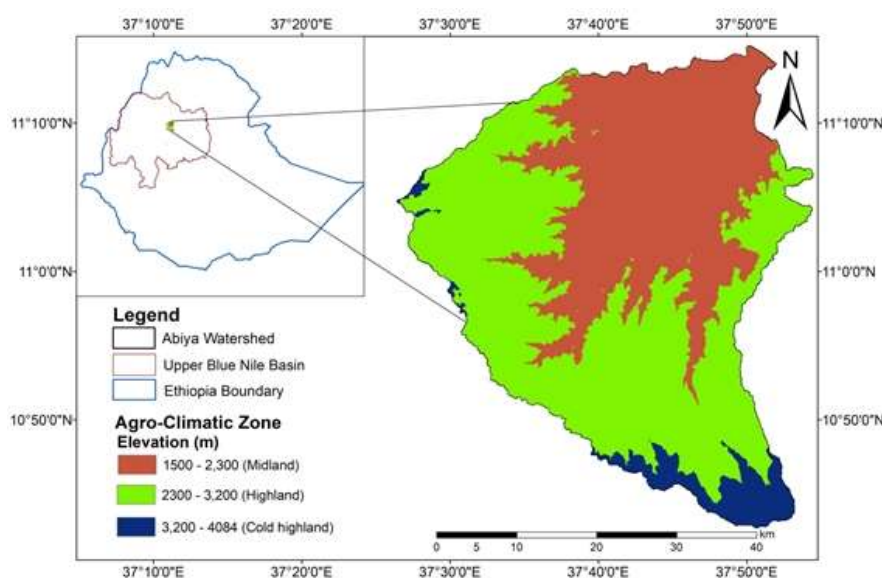


Figure 1. Location map of the agro-climatic zones (in metres) of the study area.

Geographically, the watershed is characterised by its highly undulating topography, which consists of mountains, deep gorges, escarpments, and plateaus. Most of the residents in the watershed were involved in mixed agriculture, which includes both crop cultivation and livestock rearing. In the Amhara region, where they consider the location to be arranged, the average family size is anticipated to be 4.6 individuals, whereas

the population density is expected to be 189.4 people km⁻²^[31]. Based on this, it is better to project the total population inhabiting the watershed, and the aggregate population of the area is 344,572.

3. Data and methods

This section reviews the data source used for this study and the selection and calculation of the indices. It also presents a trend examination of selected extreme rainfall indices by using Mann-Kendall's (MK) and Sen's slope statistics to estimate the trends and magnitude changes of the extreme rainfall indices, respectively.

3.1. Data

3.1.1. Digital elevation model

A digital elevation model with (30 m × 30 m resolution) was used for this study. It was accessed from the United States Geological Survey (USGS) <https://earthexplorer.usgs.gov/> for generating ACZs and calculating their area coverage (**Table 1**).

Table 1. Areal coverage of the ACZs of the Abiya watershed.

ACZs	Midland	Highland	Cold-highland	Watershed
Elevation (metres)	1500–2300	2300–3200	3200–4084	1379–4084
Area (ha)	77,057	95,527	9344	181,928
%	42.4	52.5	5.1	100

3.1.2. CHIRPS satellite data

The rainfall station databases of Ethiopia have many missing values^[28], do not have adequate data records to support trend analysis^[32], and do not make available well-timed and sufficient rainfall pattern data due to the scattering of observations, uneven allocation, and data gaps in the not-handled dataset^[33]. Accordingly, it became mandatory to employ an alternative rainfall data source. Nowadays, there are several satellite-based precipitation datasets with varying spatiotemporal resolutions that are viable alternatives to rain gauge data. CHIRPS is a comparatively new rainfall dataset with good spatial (0.05°) and temporal (daily) resolution, and it is derived from multiple data sources covering 50° S and 50° N from 1981 to the present.

At several locations throughout the world, CHIRPS has undergone validation, and the study's findings have been good. For instance, Dinku et al.^[34] assessed the execution of the CHIRPS dataset in comparison to 1200 area rain gauge measurements from Ethiopia, Kenya, and Tanzania, and they found that CHIRPS worked better than other high-resolution satellite products of the rainfall dataset in several parts of East Africa. Similarly, CHIRPS was used because of its high accuracy and best performance in Ethiopia^[35]. CHIRPS has been tested, and it works very well in different places in the country, such as Taye et al.^[36] in the upper Blue Nile basin, Ethiopia, and Alemu and Bawoke^[37] in the Amhara region, Ethiopia, respectively. In this study, the CHIRPS rainfall data was used without checking. The study area was also found under the previous validation conducted. The Abiya watershed is a micro-watershed found in the Amhara region, Upper Blue Nile basin, Ethiopia.

This study obtained 39 years (1981–2019) of record precipitation data from the CHIRPS dataset for 50 sample grid points (each representing an area of 5 km × 5 km), which was accessible online at http://climexp.knmi.nl/select.cgi?field=chirps_20_25. The entire grid points (**Figure 2**) cover the period from 1981–2019, and there were strata for three ACZs. The classification is intended to purposefully represent the rainfall conditions of each ACZ in the research area (ACZs: 21, 26, and 3 grid points correspond to the midland, highland, and cold-highland, respectively).

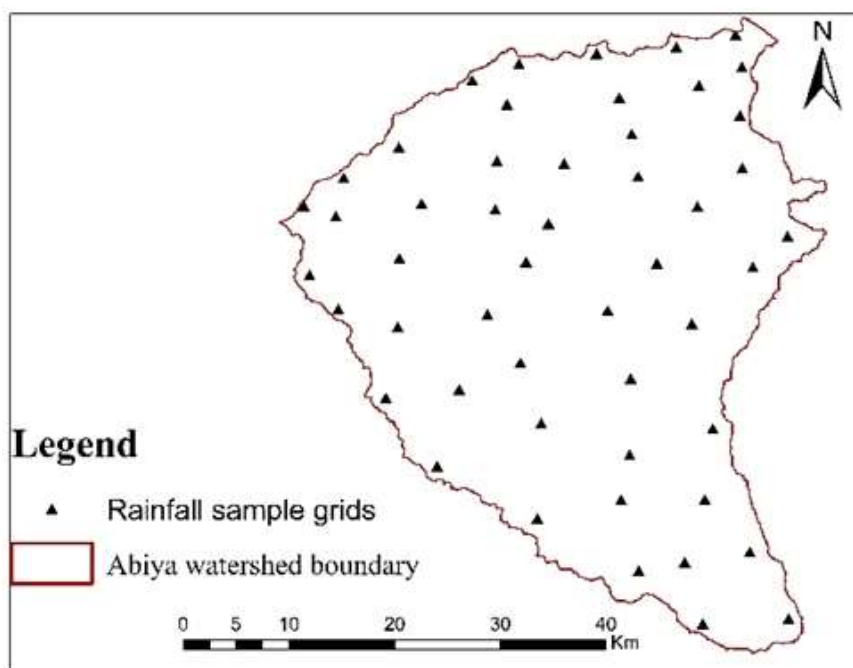


Figure 2. Sample grids were taken into consideration for gathering rainfall datasets in Abiya Watershed.

3.1.3. Local farmers

In the context of the Northwest Highlands of Ethiopia, focus group discussion (FGD) is the best way of generating primary information or data about the locality. The national database of Ethiopia is very fragmented and doesn't aggregate information at the micro-watershed or ACZ level. Accordingly, the qualitative dataset of the current study was collected using FGDs. In the three ACZs of the watershed, FGDs were conducted to determine the dominant summer cereal crops, their crop calendar, and any potential consequences of extreme rainfall on the crop calendar. One FGD was made in each ACZ, and each FGD consists of eight participants. The participants were chosen by considering their ACZs to capture their crop calendar timing and the possible consequences of extreme rainfall indices. To gather data regarding the existing climate variability, elders (>50 years old) were purposely included in the FGDs.

3.2. Methods

3.2.1. Extreme rainfall indices analysis

Eight daily extreme rainfall indices were well-defined and used, which were advanced by the Joint Commission for Climatology (CCI), the Climate Variability and Predictability (CLIVAR), and the Joint Commission for Oceanography and Marine Meteorology (JCOMM) Expert Team on Climate Change Detection and Indices (ETCCDI). A choice was established in consideration of imaginable impacts on cereal crop agriculture production over the watershed and significant references given by WMO^[38]. Additionally, indices based on absolute thresholds give better information for impact studies than indices with percentile thresholds, which are more appropriate for spatial assessment.

The three crop calendar periods (LPT, SaMT, and HaTT) that had been identified using focus group discussion and examined in this study for trends in the extreme rainfall indices, the chosen daily indices for the years 1981–2019. As shown in **Table 2**, each index was calculated using INSTAT+ software (version 3.36), which was created to simplify and analyse climatic data developed in the previous study^[39]. The selected indices were calculated in keeping with the ETCCDI instructions. http://etccdi.pacificclimate.org/list_27_indices.shtml.

Table 2. Definitions of selected extreme rainfall indices.

Indices	Name	Definitions	Unit
R × 1 day	Maximum one-day precipitation	Maximum one-day precipitation in a crop calendar	mm
R × 5 day	Maximum five-day precipitation	Maximum consecutive five-day precipitation in a crop calendar	mm
SDII	Simple daily intensity index	Mean precipitation amount on a wet day in a crop calendar, where a wet day is a day with precipitation ≥ 1 mm	mm/day
R10 mm	Heavy precipitation days	Count of days with precipitation amount ≥ 10 mm in a crop calendar	days
R20 mm	Very heavy precipitation days	Maximum count of days with precipitation amount ≥ 20 mm in a crop calendar	days
CDD	Consecutive dry days	Maximum count of consecutive days with precipitation amount < 1 mm in a crop calendar	days
CWD	Consecutive wet days	Maximum count of consecutive days with precipitation amount ≥ 1 mm in a crop calendar	days
PRCPTOT	Total precipitation on wet days	Total precipitation amount on wet days in a crop calendar	mm

3.2.2. Serial autocorrelation test

For trend detection in time series, it is necessary to have data that is random and persistence-free^[40] in order to eliminate the confounding influence of serial dependence on the interpretation of the findings. To avoid the manipulation of serial autocorrelation on the Mann-Kendal (MK) trend test, serial autocorrelation would have been looked at prior to using the MK trend test. Accordingly, in this work, the autocorrelation function as stated in the study of Von Storch^[41] was utilised to test the randomness and independence of the longitudinal rainfall data for each ACZ as follows:

$$r_k = \left[\frac{1}{n-1} \sum_{i=1}^{n-k} (X_i - \bar{X})(X_{i+k} - \bar{X}) \right] / \left[\frac{1}{n} \sum_{i=1}^n (X_i - \bar{X})^2 \right] \quad (1)$$

where r_k is the lag- k autocorrelation coefficient, \bar{X} is the mean value of a time X_i , n is the number of observations, and k is the time lag. Random series have autocorrelations close to zero for all time-lag divisions, except the zero-lag coefficient, which is always one. In that case, statistical tests are applied directly to the series. Statistical tests are employed in this scenario on a pre-whitened series to apply to non-random series that have one or more significantly non-zero autocorrelation values to account for the non-randomness^[42].

3.2.3. Mann-Kendall test (MK)

MK is a non-parametric statistical test used to discover if a series of data is going up or down. The MK test was used to detect the statistical significance of the tendencies throughout the observation^[43]. The statistical significance of the trends seen during the observation was assessed using the MK test^[44]. Earlier research by Feng et al.^[43] and Poudel and Shaw^[44] demonstrated that the test's length and the allocation of the data do not follow a predetermined pattern. It is not affected by whether some data were absent or if the intervals between measurements were unequal.

It is recognised by Feng et al.^[43] that the MK statistics S , the variance statistic $\text{Var}(\sigma)$, and the consistent standard normal test statistic Z could be considered as follows:

$$S = \sum_{i=1}^{n-1} \sum_{j=i+1}^n \text{sgn}(x_j - x_i) \quad (2)$$

where n is the length of the dataset, x_i and x_j are two elements of the measured time series at the time step i and j , respectively, and

$$\text{sgn}(x_j - x_i) = \begin{cases} -1, & (x_j - x_i) < 0 \\ 0, & (x_j - x_i) = 0 \\ 1, & (x_j - x_i) > 0 \end{cases} \quad (3)$$

If the dataset is identically and independently distributed, then the mean of S is zero, and the variance of S is given by

$$\text{Var}(S) = \frac{1}{18} n(n-1)(2n+5) - \sum_{i=1}^m t_i(t_i-1)(2t_i+5) \quad (4)$$

where n is the length of the dataset, m is the number of tied groups (a tied group is a set of sample data having the same value) in the time series, and t_i is the number of data points in the i^{th} group.

The formula is used to calculate Z statistics.

$$Z = \begin{cases} \frac{S+1}{\sqrt{\text{Var}(S)}} & \text{for } S < 0 \\ 0 & \text{for } S = 0 \\ \frac{S-1}{\sqrt{\text{Var}(S)}} & \text{for } S > 0 \end{cases} \quad (5)$$

Trends that are increasing or falling are indicated by positive or negative values Z , accordingly. A statistical significance level is employed to check the monotonic trend. The trend is statistically significant at the 99% confidence level if $(Z) > 2.58$, at the 95% confidence level if $(Z) > 1.96$, and at the 90% confidence level if $(Z) > 1.65$ ^[45].

3.2.4. Sen's slope estimator

Sen's slope estimator is a non-parametric procedure used to measure how much of a pattern there is in a set of data that changes over time. It is a more robust estimator than others because of its relative insensitivity to extreme values^[46]. Sen's slope estimator is also used to figure out the trend magnitude in hydro-meteorological time series^[47]. This method helps to lessen the impact of missed data or strange values as compared with linear regression^[37,48,49].

For a given time series $X_i = x_1, x_2, x_3, \dots, x_n$, having N pairs of data, the slope is computed as

$$\beta_i = \left(\frac{x_j - x_i}{j - i} \right), i = 1, 2, 3, \dots, N, j > i, \quad (6)$$

Sen's Slope β represents the average of the slope values β_i and is calculated as

$$\beta = \begin{cases} \frac{\beta_{N+1}}{2}, & \text{if } N \text{ is odd} \\ \left(\frac{\beta_{\frac{N}{2}} + \beta_{\frac{N+2}{2}}}{2} \right), & \text{if } N \text{ is even} \end{cases} \quad (7)$$

The sign of β reflects the figure's inclination signal, whereas its value shows the steepness of the trend^[37].

4. Results and discussion

In this study, three ACZs of the Abiya watershed were used to analyse the trend of the daily extreme rainfall indices and their consequences on the *Meher* (summer) cereal crop calendar from 1981–2019. The main crops in each ACZ in the watershed, as well as the unique crop calendar, are initially identified. Then the trends of all extreme rainfall indices in each ACZ were examined for a variety of crops, and the implications of the observed trend and the local farmers' perceptions were investigated.

4.1. Consequences of the extreme rainfall indices on the crop calendar

- Classifying crop calendar time

The main local crop calendars for cereal crop production systems were found to be LPT, SaMT, and HaTT based on the data and information collected from local farmers through FGDs. It was discovered that the primary cereal crops growing during the *Meher* (summer) season were barley (*Hordeum vulgare*) from the cold-highland region, maize (*Zea mays*) and wheat (*Triticum* spp.) from the highland region, and maize (*Zea mays*) and teff (*Eragrostis tef*) from the midland region. For a country similar to Ethiopia, where rain-fed activity is common, a study like this has significant benefits because *Meher* season crops are those that are harvested between September and February. Next, taking into account the annual optimum rainfall amounts, they precisely determined a typical period for each field operation using specific commonalities that typically occur during transitions.

The precipitation distribution in a particular year is “normal” for farmers inside the watershed. Within the event of rainfall variability, rainfall beginning, interval, offset times, quantity, and distribution together create a favourable zone for them to effectively practice all the needed crop production. The key field activities were categorised into LPT, SaMT, and HaTT, principally based on their proximity to rainfall supplies. Arrangements of weeks (first, second, third, or fourth week) of a stated month are used as the first and end dates for each farming time, as presented in **Table 3**. The identical crop calendar identification methodology was applied in previous studies by Endale et al.^[50].

Table 3. Crop calendar for the main *Meher* cereal crops in the ACZs of the study area.

ACZs	Midland		Highland		Cold-highland
Crop name	Maize	Teff	Maize	Wheat	Barley
LPT	1st week March–3rd week May	1st week March–4th week June	4th week February–1st week May	4th week February–2nd week June	1st week February–2nd week May
SaMT	4th week May–2nd week October	1st week July–3rd week October	2nd week May–1st week November	3rd week June–3rd week October	3rd week May–1st week October
HaTT	3rd week October–2nd week November	4th week October–3rd week November	2nd week November–4th week November	4th week October–2nd week November	2nd week October–1st week November

Since a week contains 7 days, local farmers were not able to accurately remember the beginning and end dates for all crops because they didn't memorise them, and it caused more or less a misconception. Local farmers believe it is fair to describe the first and end dates for each crop calendar in terms of weeks, which is crucial for this study's examination of the extreme rainfall indices. To respond to actual periods and have reliability in an analysis, the start and end dates of a defined week were used as the first and last days for that specific crop calendar, respectively. On the contrary, it doesn't entail any local farmer doing major farm field operations either initially or later than the clearly specified crop calendar time. As opposed to the LPT, SaMT, and HaTT, there were a few seasons that didn't fit into the three crop calendars (**Table 3**).

- Rainfall autocorrelation

All autocorrelations fell within 5% significance levels, and there was no apparent pattern (e.g., positive autocorrelations followed by negative autocorrelations). This means the yearly rainfall time series for all ACZs did not show any significant serial correlation at all lags. The rainfall data were not correlated with each other (**Figure 3**).

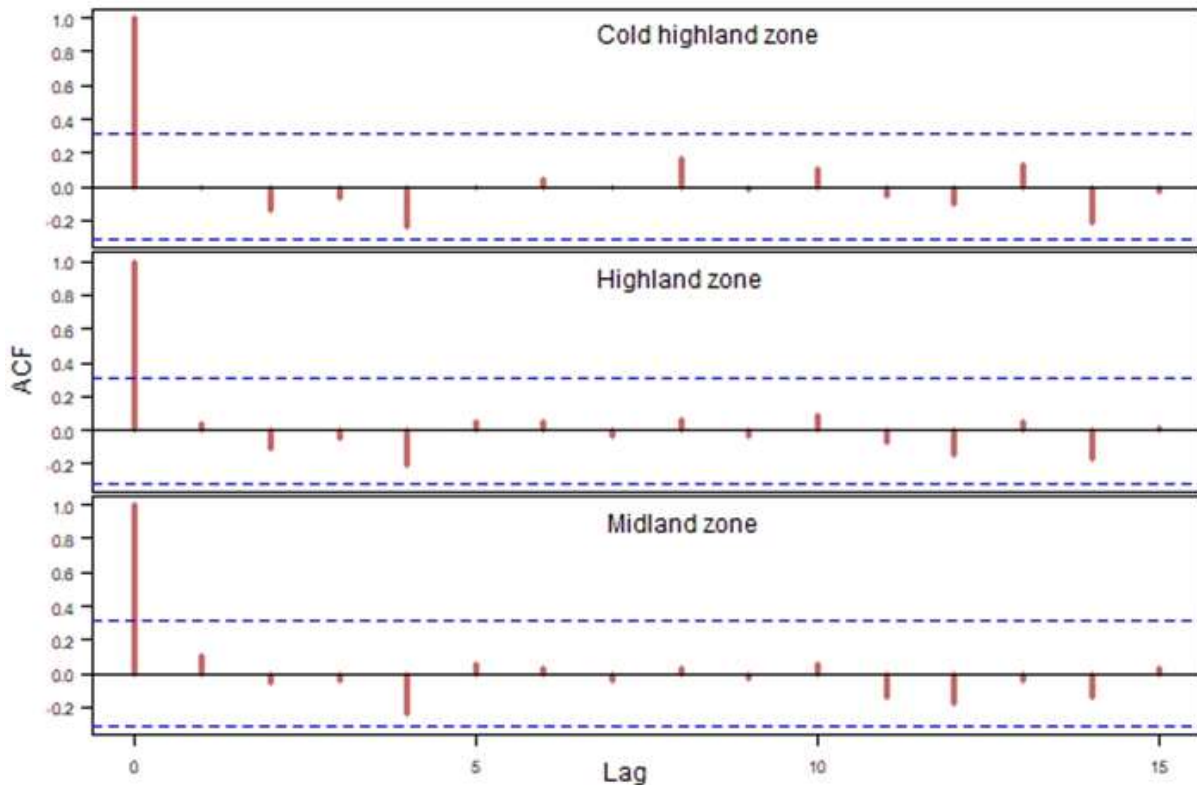


Figure 3. The correlation value of the annual rainfall at different lags in three ACZs.

This time series was random, meeting the independence distribution criteria. The results revealed that the observed rainfall series data in the Amhara region of Ethiopia did not exhibit continuous persistence, as demonstrated by other research^[29,37]. However, this non-association was the essence of randomness. In short, adjacent observations did not “correlate” (the areal average annual rainfall data indicated that no dependency or periodicity existed in this time series and suggested that areal average annual rainfall quantities are entirely independent of one year to the next). The autocorrelation function (ACF) for yearly rainfall in all ACZs showed, on the whole, no significant ongoing correlation by whole lags at the 5% significance level. Therefore, the analysis of the trends in the characteristics of the rainfall did not need any further data manipulation; the MK test was carried out directly. Outcomes from the serial correlation test, the MK test, and Sen’s slope predictor should be applied to the rainfall data from 1981–2019 for the Abiya watershed in all ACZs.

4.1.1. Trends in extreme rainfall indices at land preparation time

The trends of extreme rainfall indices for all crops in all ACZs during the LPT are given in **Table 4**. The outcomes of the MK trend tests indicated that in the study area, the highest of the indices displayed an increasing signal for 75% of the indices ($R \times 1$ day, $R \times 5$ day, SDII, R10 mm, CWD, and PRCPTOT) and descending indications for the remaining 25% of the indices (R20 mm and CDD) in the area during the LPT of teff. All observed extreme rainfall trends in LPT R10 mm were only significant at a 5% significance level.

Table 4. The trends of extreme rainfall indices for preferred cereals during LPT in each ACZ.

ACZs		Midland				
Crop name		Teff			Maize	
Name of indices	Mean	MK	Trend	Mean	MK	Trend
R × 1 day (mm)	28.05	0.65	0.05	20.72	0.45	0.03
R × 5 day (mm)	58.45	0.63	0.09	42.49	0.44	0.11
SDII (mm/day)	7.19	1.32	0.02	6.60	1.36	0.02
R10 mm (day)	9.61	2.01**	0.09	4.38	1.29	0.03
R20 mm (day)	2.05	-0.29	0.00	0.79	-0.41	0.00
CDD (day)	82.38	-0.61	-0.06	60.82	0.51	0.34
CWD (day)	38.71	0.62	0.06	20.20	-0.45	-0.03
PRCPTOT (mm)	279.38	1.26	1.39	133.75	0.54	0.34
ACZs		Highland				
Crop name		Wheat			Maize	
Name of indices	Mean	MK	Trend	Mean	MK	Trend
R × 1 day (mm)	26.04	0.12	0.01	21.48	0.34	0.04
R × 5 day (mm)	55.45	0.45	0.10	44	0.29	0.05
SDII (mm/day)	7.09	1.31	0.02	7.09	0.58	0.14
R10 mm (day)	8.02	1.78*	0.10	4.02	0.42	0.00
R20 mm (day)	1.62	0.09	0.00	0.76	0.23	0.00
CDD (day)	72.23	-1.19	-0.17	57.18	-0.27	0.00
CWD (day)	34.12	1.13	0.15	17.07	0.21	0.00
PRCPTOT (mm)	245.23	1.52	2.03	119.69	0.17	0.10
ACZs		Cold highland				
Crop name		Barley				
Name of indices	Mean	MK	Trend			
R × 1 day (mm)	26.54	-0.59	-0.07			
R × 5 day (mm)	54.52	0.54	0.17			
SDII (mm/day)	6.72	0.92	0.02			
R10 mm (day)	6.3	0.79	0.00			
R20 mm (day)	1.2	-0.10	0.00			
CDD (day)	77.59	-0.91	-0.10			
CWD (day)	27.59	0.19	0.00			
PRCPTOT (mm)	184.67	0.74	0.60			

Note: * is statistical significance at 0.1, ** is statistical significance at 0.05.

The majority, 75% of the indices, revealed rising trends with R × 1 day, R × 5 day, SDII, R10 mm, and PRCPTOT. The remaining 25% of the indices indicated a decreasing trend, with R20 mm and CWD observed during the LPT of maize. From all observed increasing and declining trends, the indices were non-significant in statistical terms during the LPT of maize at any level. CWD was decreasing, and a divergent trend in CDD was observed. Insufficient spring rainfall affects crop productivity in the main rainy season that follows by influencing soil moisture levels and long-cycle crop varieties like maize^[51]. Furthermore, the availability and lack of rainfall greater or lower than 1mm were used to measure CWD and CDD, respectively. The LPT of

maize revealed a declining trend in CWD and a rising trend in CDD. As presented by Worku et al.^[16], a decreasing inclination in CWD and a rising trend in CDD point to a worsening of the drought in the area.

For wheat during LPT, the temporal means and signs in the indices were computed at the highland zone depicted in **Table 4**. The MK trend tests in the watershed revealed a rising signal for 87.5% of the indices with $R \times 1$ day, $R \times 5$ day, SDII, R10 mm, R20 mm, CWD, and PRCPTOT and declining signals for the remaining 12.5% of the indices with CDD in the area during the LPT. Even though all of the observed trends in LPT rainfall were extreme, only R10 mm was significant at a 10% level of significance. As the results of **Table 4** show, the majority (87.5%) in the signals of the indices increased with $R \times 1$ day, $R \times 5$ day, SDII, R10 mm, R20 mm, and PRCPTOT, while decreasing for the remaining 12.5% of the CDD observed during the LPT of maize. All the observed increasing and declining inclinations of the indices were non-significant in statistical terms during the LPT of maize. Half of the extreme change was 0.00 days per decade.

The trend analyses for the LPT periods of barley during the study period in the cold-highland area did not reveal any consistent patterns, although the MK trend tests revealed going up signals for 62.5% of the indices $R \times 5$ day, SDII, R10 mm, CWD, and PRCPTOT. The downward signals for 37.5% of the indices were $R \times 1$ day, R20 mm, and CDD. Using CWD and CDD, the availability and lack of rainfall greater or lower than 1 mm were determined, respectively. As shown below, CWD was increasing and CDD was decreasing. This suggests that there is rainfall during the LPT of barley. Besides, in this study, the CWD exhibited going-up trends in all ACZs during LPT. Nevertheless, Endale et al.^[50] investigated in the *Merti* district and found a falling trend in CWD. SDII is positive, and it is suggested that the daily rainfall has been increasing. The PRCPTOT indicates a positive trend in each ACZ during the LPT. Contrary to this, a study revealed declining tendencies in PRCPTOT among varying agro-ecological zones in the tropical highlands at Choke Mountain, which is the extending part of the watershed^[52].

The trends of the indices for LPT also vary among the three ACZs. For example, R20 mm decreased in the midland and cold-highland zones while rising in the highland region. It is understood that the scales and observed effects of indices tend to differ across the three ACZs. Similarly to what was found in a former study, which was conducted in Ethiopia's moist region, a complex trend in the daily rainfall indices was seen^[53]. This study was similar to a prior study by Endale et al.^[50]. The indices were inconsistent and lacked statistical significance. For instance, information acquired from FGDs in all ACZs observed a declining rainfall during LPT, which critically limits the duration per season and the amount of time that could be spent cultivating per day due to high temperatures.

4.1.2. Trends in extreme rainfall indices at sowing and management time

Table 5 presents the trends in the indices computed for each crop in each ACZ during the SaMT. The table showed that seven out of the eight indices ($R \times 1$ day, $R \times 5$ day, SDII, R20 mm, CDD, CWD, and PRCPTOT) showed increasing trends for the SaMT of teff in the midland, while the remaining R10 mm revealed declining trends. In terms of statistics, there was no significance in any of the rising or falling indications. Some indices had no discernible variation in their rates of change (0.00 days per decade). Conversely, the CDD increased by 0.01 days/decades with a mean value of 35.64 days during the SaMT of teff. This suggests that during the past thirty years, CDD at the critical crop stage has increased. According to Berhane et al.^[26], a rise in CDD might influence crop development and productivity, particularly during the main rainy season. Additionally, previous studies by Ademe et al.^[54] observed that irregularities in the crucial rainy season influenced teff planting.

According to prior studies^[55], an increase in CDD frequency will have a significant negative impact on the time of the crop growth phase, which will impact crop growth and output. The MKs trend examinations

displayed an increasing indication for 62.5% of the indices SDII, R20 mm, and CWD; and PRCPTOT decreasing signals for 25% of the indices R × 5 day and CDD; and no visible signal for 12.5% of the indices R × 1 day for SaMT of maize. However, the trend investigation revealed that there was no statistical significance.

The extreme rainfall indices for wheat and maize (SaMT) in highland zones are also included in **Table 5**, along with their means value and trends. In the watershed, the MK trend tests revealed downward signals for 75% of the indices R × 1 day, R × 5 day, SDII, R20 mm, CDD, and PRCPTOT, and increasing signals for 25% of the indices R10 mm and CWD. The indices for the period of SaMT of wheat weren't statistically significant among all reported rising and decreasing trends in the area. In the same tables, the MK result for the SaMT of maize is also shown. Based on the observed trend test, 37.5% of them displayed increasing signals for the indices R10 mm, CWD, and PRCPTOT, and decreasing indications for the remaining 62.5%, which included R × 1 day, R × 5 day, SDII, R20 mm, and CDD during SaMT of maize. According to the observed trends in the SaMT extreme rainfall indices, only CWD was statistically significant at a 10% level of significance. The SDII has a negative trend during SaMT for both wheat and maize, similar to other indices. This means that the daily rainfall has declined.

Table 5. The trends of the extreme rainfall indices for preferred cereals during SaMT in each ACZ.

ACZ Midland						
Crop name	Teff			Maize		
Name of indices	Mean	MK	Trend	Mean	MK	Trend
R × 1 day (mm)	37.11	0.21	0.03	38.72	0.00	0.00
R × 5 day (mm)	93.81	0.02	0.00	94	-0.06	-0.01
SDII (mm/day)	10.90	0.21	0.00	10.33	0.16	0.01
R10 mm (day)	35.56	-0.36	0.00	39.89	0.66	0.04
R20 mm (day)	10.25	0.91	0.00	11.18	0.85	0.04
CDD (day)	35.64	0.01	0.01	52.35	-0.49	-0.04
CWD (day)	77.56	0.04	0.00	93.89	0.67	0.06
PRCPTOT (mm)	845.06	0.02	0.04	968.6	0.83	1.01
ACZ	Highland					
Crop name	Wheat			Maize		
Name of indices	Mean	MK	Trend	Mean	MK	Trend
R × 1 day (mm)	40.27	-0.46	-0.67	40.66	-0.24	-0.03
R × 5 day (mm)	100.79	-0.07	-0.03	100.79	-0.07	-0.03
SDII (mm/day)	11.03	-0.60	-0.01	10.31	-0.77	-0.10
R10 mm (day)	40.51	0.61	0.04	45.43	1.22	0.09
R20 mm (day)	12.53	-0.52	0.00	13.56	-0.55	0.00
CDD (day)	38.05	-0.69	-0.07	66.02	-1.42	-0.29
CWD (day)	90.17	0.76	0.07	111.38	1.84*	0.29
PRCPTOT (mm)	994.63	-0.17	-0.21	1146.15	0.68	1.12
ACZ	Cold highland					
Crop name	Barley					
Name of indices	Mean	MK	Trend			
R × 1 day (mm)	42.56	0.41	0.05			
R × 5 day (mm)	105.45	-0.16	-0.04			
SDII (mm/day)	10.76	-0.36	-0.01			
R10 mm (day)	46.26	1.03	0.07			
R20 mm (day)	14.28	0.05	0.00			
CDD (day)	45.18	-1.34	-0.18			
CWD (day)	104.13	1.27	0.15			
PRCPTOT (mm)	1118.25	0.31	0.53			

Note: * is statistical significance at 0.1.

The temporal means and signals of the extreme rainfall indices for SaMT in the cold-highland area are also shown in **Table 5**. As it was shown, during the SaMT of barley, the MK trend tests in the study revealed increasing signals for 62.5% of the indices R × 1 day, R10 mm, CWD, and PRCPTOT and descending signals for the remaining 37.5% of the indices SDII, R × 5 day, and CDD. The trend in the SDII is negative during the SaMT of barley, similar to other extreme rainfall indices. This may indicate that the daily rainfall has declined. The upward indication of R10 mm and R20 mm was seen during the SaMT of barley. According to Worku et

al.^[16], going up in these indices indicates potential risks related to flooding and soil erosion in the area. From all recorded trends during SaMT, none of the indices has become significant.

The majority of rainfall extremes, with the exception of CWD for the SaMT of maize in the highland zone, were not statistically significant. Endale et al.^[50] pointed out that while not all trends in SaMT rainfall extremes were significant, an increasing and decreasing indication might have a significant impact on rain-fed crop production. The delayed onset and early termination of rainfall, according to the FGD participants, had an impact on farming during the summer. The impacts of heavy rainfall and prolonged CDD at serious crop stage has increased in all ACZs over the past three decades, according to farmers who have observed that “the rain falls late after sowing time passes, and due to early termination of rainfall, the farmlands get dry and crops do not develop very well.” On the other hand, because of its nature, teff needs buddy character during SaMT; yet, the prolonged CDD may cause undesirable damage to teff planting. Their views somewhat matched the observed pattern at three ACZS and were in line with the extensive CDD at the midland zone for SaMT of teff and heavy rainfall.

SDII has shown a negative trend in the highlands and the cold highlands. Mohammed et al.^[56] pointed out that agricultural production is at risk due to the decreasing trends of SDII. For instance, the consequence of CDD with an equal length may be severe if it happens at the initial growing time of crops rather than at a later phase^[19]. A prior study by Chabala et al.^[57] found that though a CDD of 4 in 30 days after planting would be perceived as less significant, since its impact is aggregate, it could still be harmful to crop growth. Usually, the existence of prolonged dry times during critical growing and development stages might have a negative effect on crop productivity^[19]. During the SaMT of wheat, PRCPTOT appeared to rise in each ACZ except for the highland ACZ, with the maximum amount exhibited in all ACZ compared to other extreme rainfall. Contrary to this, a study employed in the tropical highlands at Choke Mountain, which is the extending part of the watershed, showed a decreasing trend in PRCPTOT over cool, sub-humid agro-ecological zones^[52].

According to a study by Megersa et al.^[58], rainfall inconsistency has direct or indirect consequences on agricultural production because it hinders crop growth and improvement by aggravating the proportion and distribution of hostile climate settings, reducing water supplies, and exacerbating the severity of soil erosion. The biggest issue facing Ethiopia’s agricultural sector has always been rainfall inconsistency. Local farmers schedule their planting time based on the onset time of the rainfall season; nonetheless, crop loss because of a false start to the rainy season may be a frequent problem^[59].

According to the FGDs member, a key problem found in the watershed was the inconsistency and variation in the onset and offset times rather than the amount of rainfall. The rain started late in the last weeks of June, and it stopped earlier in September. The FGDs participant also mentioned that the rainfall for the *Meher* season has been declining (expected to onset in June) and in September (the flowering stage of the *Meher* crops). Contrary, rainfall in September is vital since crops at that time are in the flowering or ripening stage and need more water for maturation.

4.1.3. Trends in extreme rainfall indices at harvesting and threshing time

The temporal means, trends, and the magnitude of change in the indices estimated for each crop in each ACZ during the HaTT are shown in **Table 6**. The trend analyses did not show a regular pattern among the recording data during the study period at the midland zone for the HaTT periods of both teff and maize. The MK trend tests revealed positive signals for 87.5% of the indices $R \times 1$ day, $R \times 5$ day, SDII, R10 mm, R20 mm, CWD, and PRCPTOT, and negative signals for 12.5% of the indices CCD for teff. Unlike other extreme rainfall indices, the trend in the CCD was negative during the HaTT of teff. This shows that the amount of daily rainfall has been increasing. The MK trend tests displayed rising signals for 75% of the indices $R \times 1$

day, R × 5 day, R10 mm, R20 mm, CWD, and PRCPTOT, as well as downward signals for 25% of the indices SDII and CDD during HaTT of maize. Due to the increased extreme rainfall indices, several issues, such as erosion of soil, agricultural damage, and waterlogging, would have an impact on how people leave rural and urban sites^[55].

During the HaTT of wheat, the trend signals were increasing for 62.5% of the indices R × 1 day, R × 5 day, SDII, R10 mm, CWD, and PRCPTOT, while decreasing for 25% of the indices R20 mm and CDD. There was no visible signal for 12.5% of the SDII indices. At a 5% level of significance, the CWD has statistically increased. Long CWD during the harvesting period was particularly adversely affecting crop production. Additionally, the mass of the indices increased, resulting in convergent signals of CDD. This suggests there was precipitation during the highland area HaTT of wheat. In the same table, the findings show the trend signals were increasing for 62.5% of the indices R × 1 day, R × 5 day, SDII, CWD, and PRCPTOT, decreasing for 25% of the indices R20 mm and CDD, and for 12.5% of the indices R20 mm, there was no visible signal during the harvesting times of maize in the highland area. However, no positive or negative signals for any kind of crop type were found in statistically significant trend testing. During the maize HaTT, none of the indices that were seen in trend testing had statistical significance.

Table 6. The trends of the extreme rainfall indices for preferred cereals during HaTT in each ACZ.

ACZ Midland						
Crop name	Teff			Maize		
Name of indices	Mean	MK	Trend	Mean	MK	Trend
R × 1 day (mm)	12.14	1.21	0.13	15.32	0.60	0.09
R × 5 day (mm)	31	0.47	0.17	41.53	0.35	0.2
SDII (mm/day)	5.54	0.57	0.02	7.4	-0.18	-0.09
R10 mm (day)	1.34	1.23	0.00	1.97	0.76	0.00
R20 mm (day)	0.18	0.39	0.00	0.51	0.20	0.00
CDD (day)	24.44	-1.40	-0.06	17.56	-1.11	-0.07
CWD (day)	6.59	1.46	0.07	6.48	1.28	0.07
PRCPTOT (mm)	39.15	1.16	0.42	51.67	0.94	0.4
ACZ Highland						
Crop name	Wheat			Maize		
Name of indices	Mean	MK	Trend	Mean	MK	Trend
R × 1 day (mm)	10.96	1.08	0.11	8.73	0.52	0.03
R × 5 day (mm)	30.68	0.44	0.94	20.5	0.87	0.14
SDII (mm/day)	5	0.00	0.00	4.38	0.11	0.00
R10 mm (day)	1.23	0.65	0.00	0.51	-1.17	0.00
R20 mm (day)	0.15	-0.12	0.00	0.00	0.00	0.00
CDD (day)	23.85	-1.55	-0.09	24.87	-1.30	-0.05
CWD (day)	7.25	1.66*	0.1	5.28	1.32	0.06
PRCPTOT (mm)	39.55	1.23	0.42	23.38	0.97	0.22
ACZs Cold highland						
Crop name	Barley					
Name of indices	Mean	MK	Trend			
R × 1 day (mm)	18.49	0.56	0.08			
R × 5 day (mm)	47.129	-0.48	-0.17			
SDII (mm/day)	7.55	0.31	0.01			
R10 mm (day)	2.41	0.21	0.00			
R20 mm (day)	0.67	0.05	0.00			
CDD (day)	15.87	-0.88	-0.05			
CWD (day)	98.79	1.02	0.07			
PRCPTOT (mm)	68.47	0.28	0.17			

Note:* is statistical significance at 0.1.

For the HaTT of barley in the cold highlands, **Table 6** also presented the mean, trends, and magnitude of change in the extreme rainfall indices. During the barley harvesting times in the area, the trend signals for 75% of the indices R × 1 day, SDII, R10 mm, R20 mm, CWD, and PRCPTOT were increasing and 25% of the indices R × 5 day and CDD were declining; however, there were no statistically significant trend tests for all

rising and descending signals for barley crop types. Most of the indices were increased, and on the other hand, the CDD decreased, which shows there was rainfall during the HaTT of barley.

The investigation of the maximum indices in all ACZs revealed a rise in these indices. To detect the availability and lack of precipitation higher or lower than 1 mm, CWD and CDD were used. An ascending trend of CWD was significant in the highland zone. CDD was insignificantly decreasing in all ACZs. All ACZs, with the exception of the highlands (maize), observed a rising pattern of R10 mm and R20 mm during HaTT. Worku et al.^[16] also pointed out that increasing indices indicated major floods and soil erosion problems in the area. During the HaTT, PRCPTOT presented a positive trend in all ACZs with a high magnitude in comparison to other extreme rainfall. Contrary to this, a study in the tropical highlands at Choke Mountain, which is the extending part of the watershed, reported a decreasing trend in PRCPTOT over cool, sub-humid agro-ecological zones^[52].

The HaTT rainfall indices found for different ACZs exhibit increased and decreased signals, which have various implications for the rain-fed agriculture production system. Except for the decreasing trend, all the observed and increasing trends in HaTT rainfall indices in the midland, highland, and cold-highland zones indicate the deteriorating process of climatic conditions for *Meher* crops at the maturity stage and harvesting and threshing operations in all ACZs. The analysis of the extreme rainfall indices displays an increased trend in most extreme rainfall indices in the entire watershed during HaTT. This trend in rainfall extremes substantiates that the rainfall trend has not been stable in the Abiya watershed. This suggests that extreme rainfall events may pose damage to socioeconomic activities and ecosystems.

Participants in FGDs across ACZs justification, which was confirmed by their responses, that happenings of extreme conditions, such as extended CWD rainfalls during HaTT, may have negative consequences on crop production, physically harm crops by making them dry and dampen and cause grains to mature earlier and later; deplete growth labour supplies; and cause tension on local farmers. Their insight was supported by the recorded trends in the extreme rainfall indices of all ACZs. Average rain is also risky for harvesting time. Earlier studies^[28,59-61] reported that rainfall occurring for the duration of the harvesting time could cause harm to crops and postpone harvesting. A study by Deressa and Hassan^[62] predicted a decline in yields per hectare's net income because of rising rainfall during the harvesting season in Ethiopia. Harvesting time may cause the shattering of crop grains, pre-harvest seed germination, and disturbances in harvesting activity. Due to the irregular rainfall distribution, up to 100% of crop losses were seen in certain areas of the West Arsi Administrative Zone, Oromia Region, Ethiopia, throughout several crop-growing years due to the uneven rainfall distribution^[63].

5. Conclusions

In the three ACZs of the Abiya watershed, this study examined the consequences of extreme rainfall indices on the local farming crop calendar. The findings revealed that the bigger the number of extreme rainfall indices, the greater the trend in the most preferred crops in each ACZ. Yet, only a few of them were statistically significant. Most of the LPT, SaMT, and HaTT observed a rising trend in the highlands, midlands, and entire ACZs, respectively. Contrary to expectations, some of the decreasing trends in the extreme rainfall indices for LPT, SaMT, and HaTT were recorded in the cold-highland, highland, and all ACZs. Even with the fact that the excess of the extreme rainfall indices isn't statistically significant. The observed rising and decreasing signals could have negative consequences for rain-fed crop production. For example, during the SaMT of teff, an increasing trend in consecutive dry days was seen in the midland. The rising trend in consecutive dry days is an indication of greater aridity and a great risk of periodic rainfall deficiencies. Due to the rising trend in very heavy precipitation days (R20 mm) and heavy precipitation days (R10 mm), the area may be facing

flooding, crop damage, and soil erosion. The severity of the extreme rainfall indices varies spatially and among cereal crops. According to the findings, it is required to develop suitable crop varieties and drought-tolerant crops, as well as establish an efficient early warning system, with the aim of lessening the negative consequences of these extreme rainfall indices on the agricultural sector.

Author contributions

Conceptualization, MAT and ATL; methodology, EAM, MAT and MMA; software, EAM; validation, MAT and MMA; formal analysis, EAM; investigation, EAM; resources, MAT; data curation, EAM and MMA; writing—original draft preparation, EAM; writing—review and editing, MAT, ATL and MMA; visualization, EAM and MMA; supervision, MAT, ATL and MMA; project administration, MAT; funding acquisition, MAT. All authors have read and agreed to the published version of the manuscript.

Acknowledgments

The authors would like to thank Bahir Dar University for covering the cost of data collection. The manuscript was edited for language by Berhanu Engidaw, Department of English Language and Literature, Bahir Dar University, Bahir Dar, Ethiopia.

Conflict of interest

The authors declare no conflict of interest.

References

1. The Intergovernmental Panel on Climate Change. Climate change 2021: The physical science basis. Available online: <https://www.ipcc.ch/report/ar6/wg1/> (accessed on 29 November 2023).
2. Power SB, Delage FP. Setting and smashing extreme temperature records over the coming century. *Nature Climate Change* 2019; 9(7): 529–534. doi: 10.1038/s41558-019-0498-5
3. Okwala T, Shrestha S, Ghimire S, et al. Assessment of climate change impacts on water balance and hydrological extremes in Bang Pakong-Prachin Buri river basin, Thailand. *Environmental Research* 2020; 186: 109544. doi: 10.1016/j.envres.2020.109544
4. Donat MG, Lowry AL, Alexander LV, et al. More extreme precipitation in the world's dry and wet regions. *Nature Climate Change* 2016; 6(5): 508–513. doi: 10.1038/nclimate2941
5. Schneider S, Sarukhan J, Adejuwon J, et al. Overview of impacts, adaptation, and vulnerability to climate change. In: McCarthy JJ, Canziani OF, Leary NA, et al. (editors). *Climate Change 2001: Impacts, Adaptation, and Vulnerability*. Cambridge University Press; 2001. pp. 75–103.
6. Omondi PA, Awange JL, Forootan E, et al. Changes in temperature and precipitation extremes over the Greater Horn of Africa region from 1961 to 2010. *International Journal of Climatology* 2014; 34(4): 1262–1277. doi: 10.1002/joc.3763
7. Hoegh-Guldberg O, Jacob D, Taylor M, et al. Impacts of 1.5 °C global warming on natural and human systems. In: Masson-Delmotte V, Zhai P, Pörtner HO, et al. (editors). *Global warming of 1.5 °C: An IPCC Special Report on the Impacts of Global Warming of 1.5 °C above Pre-Industrial Levels and Related Global Greenhouse Gas Emission Pathways, in the Context of Strengthening the Global Response to the Threat of Climate Change*. Intergovernmental Panel on Climate Change; 2019. pp. 175–311.
8. Liebmann B, Hoerling MP, Funk C, et al. Understanding recent eastern Horn of Africa rainfall variability and change. *Journal of Climate* 2014; 27(23): 8630–8645. doi: 10.1175/JCLI-D-13-00714.1
9. Lyon B. Seasonal drought in the Greater Horn of Africa and its recent increase during the March–May long rains. *Journal of Climate* 2014; 27(21): 7953–7975. doi: 10.1175/JCLI-D-13-00459.1
10. Yang W, Seager R, Cane MA, Lyon B. The East African long rains in observations and models. *Journal of Climate* 2014; 27(19): 7185–7202. doi: 10.1175/JCLI-D-13-00447.1
11. Omambia AN, Shemsanga C, Hernandez IAS. Climate change impacts, vulnerability, and adaptation in East Africa (EA) and South America (SA). In: Chen WY, Seiner J, Suzuki T, Lackner M (editors). *Handbook of Climate Change Mitigation and Adaptation*. Springer; 2012. pp. 749–799. doi: 10.1007/978-3-319-14409-2_17
12. Dile YT, Tekleab S, Ayana EK, et al. Advances in water resources research in the Upper Blue Nile basin and the way forward: A review. *Journal of Hydrology* 2018; 560: 407–423. doi: 10.1016/j.jhydrol.2018.03.042

13. Jothimani M, Abebe A, Dawit Z. Mapping of soil erosion-prone sub-watersheds through drainage morphometric analysis and weighted sum approach: A case study of the Kulfo River basin, Rift valley, Arba Minch, Southern Ethiopia. *Modeling Earth Systems and Environment* 2020; 6: 2377–2389. doi: 10.1007/s40808-020-00820-y
14. Mohammed JA, Gashaw T, Tefera GW, et al. Changes in observed rainfall and temperature extremes in the Upper Blue Nile Basin of Ethiopia. *Weather and Climate Extremes* 2022; 37: 100468. doi: 10.1016/j.wace.2022.100468
15. Worqlul AW, Dile YT, Ayana EK, et al. Impact of climate change on streamflow hydrology in headwater catchments of the Upper Blue Nile Basin, Ethiopia. *Water* 2018; 10(2): 120. doi: 10.3390/w10020120
16. Worku G, Teferi E, Bantider A, Dile YT. Observed changes in extremes of daily rainfall and temperature in Jemma Sub-Basin, Upper Blue Nile Basin, Ethiopia. *Theoretical and Applied Climatology* 2019; 135: 839–854. doi: 10.1007/s00704-018-2412-x
17. Mengistu D, Bewket W, Lal R. Recent spatiotemporal temperature and rainfall variability and trends over the Upper Blue Nile River Basin, Ethiopia. *International Journal of Climatology* 2014; 34(7): 2278–2292. doi: 10.1002/joc.3837
18. Mika J. Changes in weather and climate extremes: Phenomenology and empirical approaches. *Climatic Change* 2013; 121(1): 15–26. doi: 10.1007/s10584-013-0914-1
19. Yu H, Zhang Q, Sun P, Song C. Impact of droughts on winter wheat yield in different growth stages during 2001–2016 in Eastern China. *International Journal of Disaster Risk Science* 2018; 9: 376–391. doi: 10.1007/s13753-018-0187-4
20. Panda DK, Mishra A, Kumar A, et al. Spatiotemporal patterns in the mean and extreme temperature indices of India, 1971–2005. *International Journal of Climatology* 2014; 34(13): 3585–3603. doi: 10.1002/joc.3931
21. Libanda B. Multi-model synthesis of future extreme temperature indices over Zambia. *Modeling Earth Systems and Environment* 2020; 6(2): 743–757. doi: 10.1007/s40808-020-00734-9
22. Tierney JE, Smerdon JE, Anchukaitis KJ, Seager R. Multidecadal variability in East African hydroclimate controlled by the Indian Ocean. *Nature* 2013; 493(7432): 389–392. doi: 10.1038/nature11785
23. Wu C, Huang G, Yu H, et al. Spatial and temporal distributions of trends in climate extremes of the Feilaixia catchment in the upstream area of the Beijiang River Basin, South China. *International Journal of Climatology* 2014; 34(11): 3161–3178. doi: 10.1002/joc.3900
24. Megersa G, Tesfaye K, Getnet M, et al. Rainfall variability and its implications for wheat and barley production in central Ethiopia. *Ethiopian Journal of Crop Science* 2019; 7(2): 89–111.
25. Geremew GM, Mini S, Abegaz A. Spatiotemporal variability and trends in rainfall extremes in Enebsie Sar Midir district, northwest Ethiopia. *Modeling Earth Systems and Environment* 2020; 6: 1177–1187. doi: 10.1007/s40808-020-00749-2
26. Berhane A, Hadgu G, Worku W, Abrha B. Trends in extreme temperature and rainfall indices in the semi-arid areas of Western Tigray, Ethiopia. *Environmental Systems Research* 2020; 9(1): 1–20. doi: 10.1186/s40068-020-00165-6
27. Dinku T, Hailemariam K, Maidment R, et al. Combined use of satellite estimates and rain gauge observations to generate high-quality historical rainfall time series over Ethiopia. *International Journal of Climatology* 2014; 34(7): 2489–2504. doi: 10.1002/joc.3855
28. Asfaw A, Simane B, Hassen A, Bantider A. Variability and time series trend analysis of rainfall and temperature in northcentral Ethiopia: A case study in Woleka sub-basin. *Weather and Climate Extremes* 2018; 19: 29–41. doi: 10.1016/j.wace.2017.12.002
29. Ayalew D, Tesfaye K, Mamo G, et al. Variability of rainfall and its current trend in Amhara region, Ethiopia. *African Journal of Agricultural Research* 2012; 7(10): 1475–1486. doi: 10.5897/AJAR11.698
30. Ministry of Agriculture (MoA). *Agro-Ecological Zonation of Ethiopia*. Ministry of Agriculture (MoA); 2000.
31. Bureau of Finance and Economic Development (BoFED). *Population Affaires Core Process Based on 2012 Inter-Censal Survey: Amhara National Regional State Development Indicator*. Bureau of Finance and Economic Development (BoFED); 2014. p. 15.
32. Alemayehu A, Bewket W. Determinants of smallholder farmers’ choice of coping and adaptation strategies to climate change and variability in the central highlands of Ethiopia. *Environmental Development* 2017; 24: 77–85. doi: 10.1016/j.envdev.2017.06.006
33. Fenta AA, Yasuda H, Shimizu K, et al. Evaluation of satellite rainfall estimates over the Lake Tana basin at the source region of the Blue Nile River. *Atmospheric Research* 2018; 212: 43–53. doi: 10.1016/j.atmosres.2018.05.009
34. Dinku T, Funk C, Peterson P, et al. Validation of the CHIRPS satellite rainfall estimates over eastern Africa. *Quarterly Journal of the Royal Meteorological Society* 2018; 144: 292–312. doi: 10.1002/qj.3244
35. Lemma E, Upadhyaya S, Ramsankaran RA. Investigating the performance of satellite and reanalysis rainfall products at monthly timescales across different rainfall regimes of Ethiopia. *International Journal of Remote Sensing* 2019; 40(10): 4019–4042. doi: 10.1080/01431161.2018.1558373

36. Taye M, Sahlu D, Zaitchik BF, Neka M. Evaluation of satellite rainfall estimates for meteorological drought analysis over the upper Blue Nile basin, Ethiopia. *Geosciences* 2020; 10(9): 352. doi: 10.3390/geosciences10090352
37. Alemu MM, Bawoke GT. Analysis of spatial variability and temporal trends of rainfall in Amhara region, Ethiopia. *Journal of Water and Climate Change* 2020; 11(4): 1505–1520. doi: 10.2166/wcc.2019.084
38. Albert MG, Tank K, Zwiers FW, Zhang X. *Guidelines on Analysis of Extremes in a Changing Climate in Support of Informed Decisions for Adaptation*. World Meteorological Organization; 2009. 52p.
39. Stern R, Rijks D, Dale I, Knock J. *INSTAT Climatic Guide*. University of Reading; 2006.
40. Ngongondo C, Xu CY, Gottschalk L, Alemaw B. Evaluation of spatial and temporal characteristics of rainfall in Malawi: A case of data scarce region. *Theoretical and Applied Climatology* 2011; 106: 79–93. doi: 10.1007/s00704-011-0413-0
41. Von Storch H. Misuses of statistical analysis in climate research. In: Storch H, Navarra A (editors). *Analysis of Climate Variability: Applications of Statistical Techniques*. Springer; 1999. pp. 11–26. doi: 10.1007/978-3-662-03744-7_2
42. Fiwa L, Vanuytrecht E, Wiyo KA, Raes D. Effect of rainfall variability on the length of the crop growing period over the past three decades in central Malawi. *Climate Research* 2014; 62(1): 45–58. doi: 10.3354/cr01263
43. Feng G, Cobb S, Abdo Z, et al. Trend analysis and forecast of precipitation, reference evapotranspiration, and rainfall deficit in the Blackland Prairie of Eastern Mississippi. *Journal of Applied Meteorology and Climatology* 2016; 55(7): 1425–1439. doi: 10.1175/JAMC-D-15-0265.1
44. Poudel S, Shaw R. The relationships between climate variability and crop yield in a mountainous environment: A case study in Lamjung District, Nepal. *Climate* 2016; 4(1): 13. doi: 10.3390/cli4010013
45. Mandale VP, Mahale DM, Nandgude SB, et al. Spatio-temporal rainfall trends in Konkan region of Maharashtra State. *Advanced Agricultural Research & Technology Journal* 2017; 1(1): 61–69.
46. Chattopadhyay S, Edwards DR. Long-term trend analysis of precipitation and air temperature for Kentucky, United States. *Climate* 2016; 4(1): 10. doi: 10.3390/cli4010010
47. Jain SK, Kumar V. Trend analysis of rainfall and temperature data for India. *Current Science* 2012; 102(1): 37–49.
48. Mekonen AA, Berlie AB. Spatiotemporal variability and trends of rainfall and temperature in the Northeastern Highlands of Ethiopia. *Modeling Earth Systems and Environment* 2020; 6: 285–300. doi: 10.1007/s40808-019-00678-9
49. Bayable G, Amare G, Alemu G, Gashaw T. Spatiotemporal variability and trends of rainfall and its association with Pacific Ocean Sea surface temperature in West Harerge Zone, Eastern Ethiopia. *Environmental Systems Research* 2021; 10(1): 1–21. doi: 10.1186/s40068-020-00216-y
50. Endale BW, Simphiwe EM, Yimer AA. Trends in climate extremes at local farming calendar timescale: Evidence from Merti District, Ethiopia. *Modeling Earth Systems and Environment* 2021; 7: 2329–2339. doi: 10.1007/s40808-020-00977-6
51. Gummadi S, Rao KP, Seid J, et al. Spatio-temporal variability and trends of precipitation and extreme rainfall events in Ethiopia in 1980–2010. *Theoretical and Applied Climatology* 2018; 134(3–4): 1315–1328. doi: 10.1007/s00704-017-2340-1
52. Birhan DA, Zaitchik BF, Fantaye KT, et al. Observed and projected trends in climate extremes in a tropical highland region: An agroecosystem perspective. *International Journal of Climatology* 2022; 42(4): 2493–2513. doi: 10.1002/joc.7378
53. Kebede G, Bewket W. Variations in rainfall and extreme event indices in the wettest part of Ethiopia. *SINET: Ethiopian Journal of Science* 2009; 32(2): 129–140. doi: 10.4314/sinet.v32i2.68864
54. Ademe D, Zaitchik BF, Tesfaye K, et al. Climate trends and variability at adaptation scale: Patterns and perceptions in an agricultural region of the Ethiopian Highlands. *Weather and Climate Extremes* 2020; 29: 100263. doi: 10.1016/j.wace.2020.100263
55. Wubaye GB, Gashaw T, Worqlul AW, et al. Trends in rainfall and temperature extremes in Ethiopia: Station and agro-ecological zone levels of analysis. *Atmosphere* 2023; 14(3): 483. doi: 10.3390/atmos14030483
56. Mohammed Y, Yimer F, Tadesse M, Tesfaye K. Variability and trends of rainfall extreme events in north east highlands of Ethiopia. *International Journal of Hydrology* 2018; 2(5): 594–605. doi: 10.15406/ijh.2018.02.00131
57. Chabala LM, Kuntashula E, Kaluba P. Characterization of temporal changes in rainfall, temperature, flooding hazard and dry spells over Zambia. *Universal Journal of Agricultural Research* 2013; 1(4): 134–144. doi: 10.13189/ujar.2013.010403
58. Megersa G, Tesfaye K, Getnet M, Tana T. Rainfall Variability and its implications for wheat and barley production in Central Ethiopia. *Ethiopian Journal of Crop Science* 2019; 7(2): 89–111.
59. Kassie BT, Hengsdijk H, Rötter R, et al. Adapting to climate variability and change: Experiences from cereal-based farming in the Central Rift and Kobo Valleys, Ethiopia. *Environmental Management* 2013; 52(5): 1115–1131. doi: 10.1007/s00267-013-0145-2

60. van der Velde M, Tubiello FN, Vrieling A, Bouraoui F. Impacts of extreme weather on wheat and maize in France: Evaluating regional crop simulations against observed data. *Climatic Change* 2012; 113(3–4): 751–765. doi: 10.1007/s10584-011-0368-2
61. Deressa TT, Hassan RM. Economic impact of climate change on crop production in Ethiopia: Evidence from cross-section measures. *Journal of African Economies* 2009; 18(4): 529–554. doi: 10.1093/jae/ejp002
62. Teklewold A, Mamo G, Admassu H. Impacts of climate change on crop production in Ethiopia. In: Mahoo H, Radeny M, Kinyangi J, Cramer L (editors). *Climate Change Vulnerability and Risk Assessment of Agriculture and Food Security in Ethiopia: Which Way Forward?* CGIAR Research Program on Climate Change, Agriculture and Food Security; 2013. pp. 13–44.
63. Evangelista P, Young N, Burnett J. How will climate change spatially affect agriculture production in Ethiopia? Case studies of important cereal crops. *Climatic Change* 2013; 119(3): 855–873. doi: 10.1007/s10584-013-0776-6